Artificial neural network-based predictive control for three-phase inverter systems with RLC filters

Iftissen Nabil[1], Ali Dali[2], Samir Abdelmalek[3]
[1]Advanced Electronic Systems Laboratory (AESL), Medea, Algeria
[2]Renewable Energy Development Centre (CDER) BP 62 Route de l'Observatoire, Algiers, Algeria
[3]National School of Nanoscience and Nanotechnology, Algiers, Algeria

Article Info

ABSTRACT

Model predictive control (MPC) is becoming more and more popular in power electronics applications, yet its practical implementation faces challenges due to computational complexity and resource demands. To address these issues, a novel MPC control approach using an artificial neural network (ANN-MPC) is put forth in this research. Using a real-time circuit modeling environment, a power converter with a virtual MPC controller that can regulate both linear and nonlinear loads is first created and run. The input-output data gathered from the virtual MPC is then used to train an artificial neural network (ANN) offline, enabling a simplified mathematical representation that significantly reduces computational complexity. Moreover, the ANN-MPC controller's adaptability to input variations enhances robustness against system uncertainties. We offer a thorough explanation of the ANN-MPC's fundamental idea, ANN architecture, offline training approach, and online functioning. The suggested controller is validated by simulation with MATLAB/Simulink tools. Performance evaluation of the novel MPC-ANN controller is performed across various scenarios, including linear and nonlinear loads under various operational conditions, and a comparative analysis with conventional MPC is presented.

Corresponding Author:

Iftissen Nabil
Advanced Electronic Systems Laboratory (AESL)
Medea, Algeria
Email: iftissen.nabil@univ-medea.dz

1. INTRODUCTION

The improved power converter efficiency has driven their widespread use across many industrial power applications. Notably, three-phase inverters are indispensable in contemporary power networks for converting DC to AC, serving critical roles in industrial settings such as motor drives, renewable energy integration, and grid-tied systems due to their efficient handling of high-power levels and reliable performance. Renewable energy sources like wind and solar can be smoothly integrated into the electrical grid thanks to advanced power electronic systems, ensuring stable and efficient power delivery. Figure 1 depicts the topology of a voltage source inverter (VSI) connected to a three-phase load with an RLC filter used to suppress harmonic distortion, thus improving the quality of the output waveform. hysteresis regulation [1], proportional-integral (PI) controller [2], active disturbance rejection control (ADRC) [3], proportional-resonant (PR) control [4], adaptive techniques [5], and model-based predictive control (MPC) [6]. There are a few of the most commonly employed control systems in power converters.

Model predictive control (MPC) enables real-time assessment of system states, leading to robust and highly efficient control in power converters. Typically, MPC consists of three main elements: a predictive

model capturing system dynamics, a reference trajectory, and an optimal controller derived through rolling optimization [7]-[10]. Despite its effectiveness in industrial applications, MPC still has limitations. Researchers have long explored methods to reduce the computational complexity of model predictive control (MPC) in power converter applications. Several strategies have been developed to overcome the high computational demands associated with MPC implementation. For instance, [11] introduces an explicit MPC approach that shifts optimization offline using multiparametric programming, significantly lowering real-time processing requirements. Another study [12] enhances prediction accuracy by proposing a discrete-time model for induction machines with time-varying parameters. Additionally, [13] combines finite control set MPC (FCS-MPC) with system identification techniques to improve performance. To further reduce computational load without sacrificing control benefits, [14] presents a simplified optimal-switching-sequence MPC (OSS-MPC) strategy. Additionally, an MPC implementation with a two-step prediction approach was introduced [15]. The computational difficulties of MPC in high-frequency power converters have yet to be universally solved, despite these attempts.

In power electronics and motor control, artificial neural networks (ANNs) are driving significant advancements in control strategies. These data-driven techniques excel at a critical task: mapping inputs to desired outputs. Researchers are even combining ANNs with established methods like model predictive control to create even more powerful approaches, such as DeepMPC [16]. This combination has shown success in real-world applications, with one study using deep neural networks to effectively control complex resonant power converters in industrial settings [17]. Another approach using ANN for the three-phase inverters [18] and multilevel inverters are discussed in [19], [20]. Liu *et al.* [21] proposed a novel technique that relies on data analysis to calculate capacitor voltages, thus eliminating the need for sensors in the system. Simonetti *et al.* [22] also suggest using the ANN-based MPC for CHB converters. ANN controllers offer distinct advantages compared to other control techniques. Key advantages include the ability to operate without requiring an exact mathematical model of the controlled system, effectively treating it as a black box.

The application of artificial neural networks (ANNs) in power electronics remains an underexplored area with significant innovation potential. This paper provides a comprehensive overview of techniques designed to address predictive control computation challenges, with a particular emphasis on the recent advancements in ANN-based model predictive control (ANN-MPC). The paper focuses on ANN-MPC applications in three-phase inverter control, assessing how this approach tackles unique implementation challenges while improving overall control efficacy.

This paper is organized as follows: i) Section 1 presents a comprehensive introduction to the research topic and provides necessary background information; ii) Section 2 presents a detailed study of the model predictive control (MPC), including the mathematical formulation of a three-phase voltage source inverter with an integrated RLC filter. This is followed by a detailed explanation of the novel ANN-MPC approach; iii) Section 3 focuses on the practical implementation of the proposed control approach, simulation studies, and an in-depth analysis of the achieved results; Finally, iv) Section 4 summarizes the results and draws conclusions based on the study.

2. METHOD

2.1. Model predictive control

Model predictive control (MPC) is an advanced control paradigm that enables multivariable system regulation through predictive optimization. The methodology utilizes either analytical or data-derived system representations to forecast dynamic behavior across a finite time horizon, Figure 1 gives this concept. In power converters, MPC optimizes switching states to achieve the desired outcome while adhering to limitations. The key steps within MPC involve prediction and optimization. Notably, the specific technique mentioned, FCS-MPC, keeps each switch in a constant ON or OFF state for a sampling period.

2.1.1. System modelling

The power stage consists of a three-phase voltage-source inverter (VSI) utilizing six IGBT switching devices with a DC bus voltage input. As illustrated in Figure 1, the output stage incorporates an RLC filter for waveform conditioning. In the system, "L" stands for the filter inductor, "C" for the filter capacitor, and "R" for the filter resistor. In the filter inductor, 'i_0' indicates the output current, 'v_c' the output voltage, and 'i_f' is the input current. V_{dc}. is the symbol for the voltage across the DC-link. The inverter's operational state is indicated by the ON-OFF status (S_a, S_b S_c) of the three transistors in the upper bridge branch. Consider the transistor's ON state to be 1 and its OFF state to be 0.

One way to express the switching state vector 'S' is as (1).

$$S = 2/3(S_a + \alpha S_b + \alpha^2 S_c) \tag{1}$$

Where $\alpha = e^{j(\frac{2\pi}{3})}$. The inverter output voltage's space vector sum is defined as (2).

$$V_i = 2/3\ (V_{aN} + \alpha V_{bN} + \alpha^2 V_{cN}) \tag{2}$$

In the context of the system V_{aN}, V_{bN} and V_{cN} represent the inverter's phase voltages in relation to the neutral point in accordance with a negative potential. The load voltage vector V_i and the switching state vector S may be related using (3).

$$V_i = V_{dc}S \tag{3}$$

Starting from the on-off states of the upper arm of the bridge and (1) and (3), we observe that we have 8 combinations of ON-OFF states that can be indicated with V_i: that is V_0 (000), V_1 (100), V_2 (110), V_3 (010), V_4 (011), V_5 (001), V_6 (101), V_7 (111). As shown in Figure 2, this vector space comprises six active vectors (V_1-V_6) and two zero vectors (V_0, V_7) that generate null output voltage.
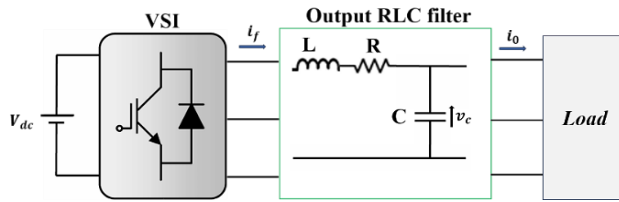
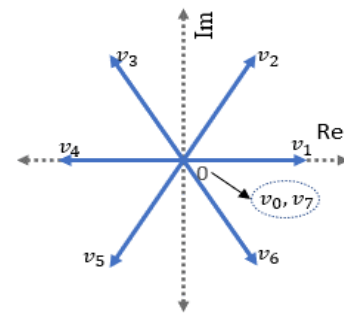Figure 1. Feeding an output RLC filter with a three-phase inverter

Figure 2. Potential voltage vectors that the inverter may produce

2.1.2. RLC filter modeling

The following are the space vectors that represent the current filter "i_f" , output voltage "v_c" and output current "i_0" using notation, as (4)-(6).

$$i_f = 2/3(i_{fa} + ai_{fb} + a^2 i_{fc}) \tag{4}$$

$$v_c = 2/3\ (v_{ca} + av_{cb} + a^2 v_{cc}) \tag{5}$$

$$i_0 = 2/3\ (i_{0a} + ai_{0b} + a^2 i_{0c}) \tag{6}$$

In the design of the RLC filter for this project, there are two main components. The effects of the variable inductance and the varying capacitor are defined by (7) and (8), respectively.

$$L\frac{di_f}{dt} = v_i - v_c - Ri_f \tag{7}$$

$$C\frac{dv_c}{dt} = i_f - i_0 \tag{8}$$

These (7) and (8) can be rewritten as (9).

$$\frac{dx}{dt} = Ax + Bv_i + Ci_0 \tag{9}$$

with : $X = \begin{bmatrix} i_f \\ v_c \end{bmatrix}$; $A = \begin{bmatrix} -R/L & \frac{-1}{L} \\ \frac{1}{C} & 0 \end{bmatrix}$; $B = \begin{bmatrix} \frac{1}{L} \\ 0 \end{bmatrix}$; $C = \begin{bmatrix} 0 \\ \frac{-1}{C} \end{bmatrix}$

The system's output is the output voltage "v_c ", The following is an expression for the state equation, as (10).

$$v_c = [0\ 1]X \tag{10}$$

From (9), with the help of the sampling time T_s, yields the discrete-time modeling of the filter, which is represented as (11).

$$X(K + 1) = A_d X(K) + B_d v_i(K) + C_d i_0(K) \tag{11}$$

With $X(K + 1) = \begin{bmatrix} i_f(K + 1) \\ v_c(K + 1) \end{bmatrix}$; $X(k) = \begin{bmatrix} i_f(K) \\ v_c(K) \end{bmatrix}$; $A_d = e^{AT_s}$; $B_d = e^{A\tau}Bd\tau$; $C_d = e^{A\tau}Cd\tau$

To estimate the output voltage v_c at time K+1, it is essential to know the capacitor voltage v_c, the inductor current i_f, and the output current i_0, all at time K. The current i_0 can be obtained either through direct measurement or by estimation using (12), which is derived from (8). In this study, we opt for direct measurement of the output current i_0 to ensure reliable and practical results.

$$i_0(K) = i_f(K - 1) - \frac{c}{T_s}(v_c(K) - v_c(K - 1)) \tag{12}$$

2.1.3. Cost function

The cost function g_N is used to identify the best switching state among seven potential anticipated output voltage vectors in order to minimize the discrepancy between the reference voltage at time k+1 and the inverter's predicted output voltage for the subsequent sampling interval. As a result, the formal expression for the cost function g_N is as (13).

$$g_N = |v_{c\alpha} * (K + 1) - v_{c\alpha}(K + 1)| + |v_{c\beta} * (K + 1) - v_{c\beta}(K + 1)| \tag{13}$$

With $v_{c\alpha} * (K + 1), v_{c\beta} * (K + 1)$, depicting the real and imaginary parts of the reference output voltage $v_c *$. $v_{c\alpha}(K + 1), v_{c\beta}(K + 1)$ are the real and imaginary parts of the predicted voltage v_c. The basic operating principle of the MPC is depicted in Figure 3.
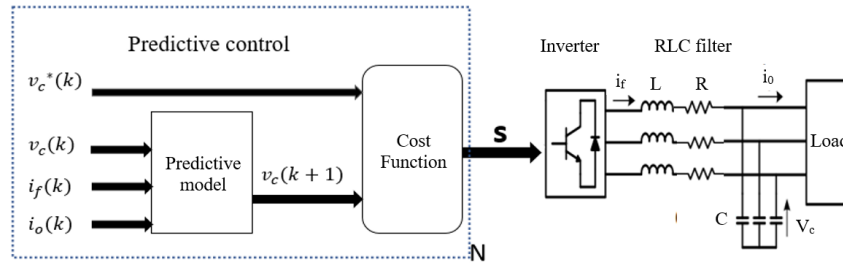

Figure 3. Block diagram illustrating the model predictive control of UPS

2.2. Concept of ANN-MPC

Artificial neural networks (ANNs), composed of fully connected layers, are highly adaptable tools capable of solving a wide range of problems, including classification tasks. When a control problem is framed as a classification task, ANNs can produce control actions that are comparable to those generated by Finite control set model predictive control (FCS-MPC) [23]-[25]. The performance of the network is strongly influenced by the size of the hidden layers. Generally, within an appropriate range, increasing the network size enhances its classification capability. In the final layer, a SoftMax activation function is applied to compute the probability associated with each possible switching state.

2.2.1. ANN training

The ANN undergoes an iterative offline training process, as illustrated in Figure 4. To begin, a power converter is designed and used with a conventional model predictive control. The input data ($[v_c(K), i_f(K)$, $i_o(K), v_c * (K)]$) and output data [S_a, S_b, S_c] from this controller are collected to serve as input and target values, respectively, for the ANN-MPC training set. The training set needs to encompass a broad range of scenarios, spanning from no load to maximum load conditions. This involves conducting numerous experiments

to generate a collection of training datasets, resulting in 108 different scenarios. These scenarios are categorized into 84 cases, each corresponding to specific resistive load values (particularly for R values). Moreover, 24 experiments are dedicated to investigating scenarios where the inverter supplies power directly to a nonlinear load, such as a diode bridge rectifier. This configuration involves varying values of nonlinear load resistance (RNL) and capacitance (CNL). Including reference voltage considerations, these simulations cover various operational situations with distinct sampling times (T_s), filter capacitance (C) and filter inductance (L) values, as well as DC link voltage (V_{dc}) and variable simulation times measured in the number of output voltage cycles. Subsequently, ANN is trained offline using the recorded samples. Throughout training phase, ANN utilizes the recorded data ($[v_c(K), i_f(K), i_0(K), v_c * (K)]$) to estimate the control signals.

Figure 5 illustrates the simulation carried out in MATLAB Simulink. The outputs generated by the Neural Network block are sent to block 1, whose objective is to fix the values using a saturation block. The optimized signals are then processed and sent to a block responsible for generating the commands for the inverter switches, as shown in Figure 6. These commands are then used by an inverter made up of six IGBT switches, whose role is to convert the DC voltage into an AC voltage to supply the load. This part has already been described step by step in section 2.1.1. Downstream of the inverter, a passive RLC filter is inserted in order to attenuate the harmonic components of the output voltage and to ensure a sinusoidal waveform that complies with power quality standards. The parameters and modeling of this filter are described in section 2.1.2.
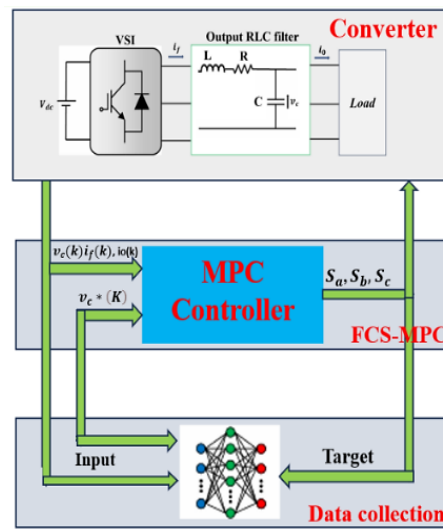

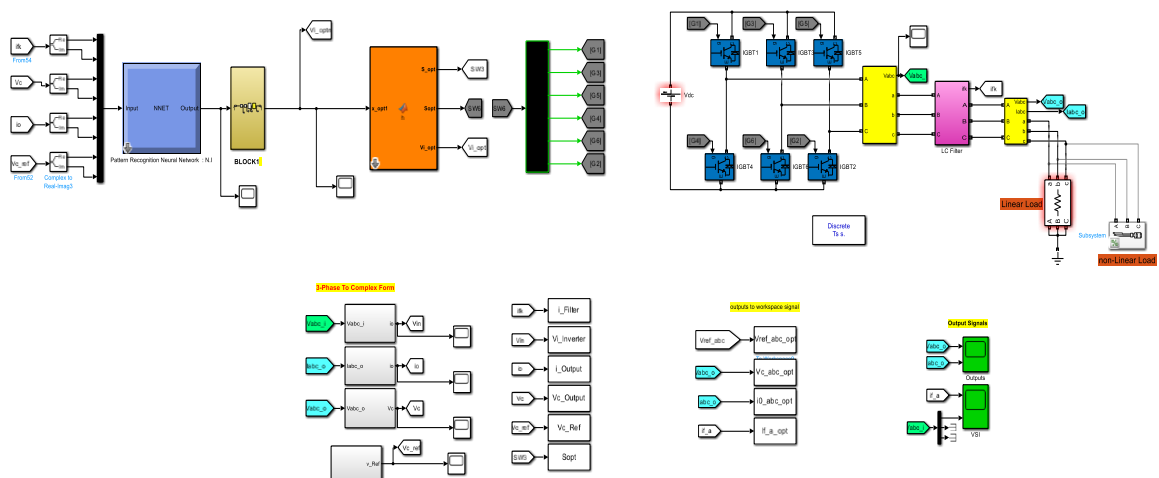Figure 4. Block of the ANN-MPC's offline training procedure

Figure 5. Block simulation

2.2.2. Enhanced ANN-base controller

The training phase and the implementation (or testing) phase are the two primary steps of the ANN-MPC control technique. The data produced by the MPC controller is used to train the Artificial Neural Network during the first offline training phase. This data also forms the foundation for gathering training, validation, and test datasets. The network is used in real-time to regulate the inverter after it has been appropriately trained and optimized. Figure 6 displays the block diagram of the ANN-based control system connected to a three-phase inverter with an RLC filter at the output. The objective is to create a high-quality sinusoidal output voltage with minimal total harmonic distortion (THD) to guarantee compliance with a variety of load scenarios.

The flowchart in Figure 7 shows the process of training and validating an artificial neural network (ANN) model. The process begins by defining the input and output parameters for the artificial neural network (ANN). Once the parameters are defined, the architecture of the ANN is designed. Following this, the ANN is trained using the defined architecture. After training, the process reaches the first decision point, where the statistical index is evaluated. If the statistical index is not acceptable, the process returns to the training phase to improve the model. If the statistical index is acceptable, the process proceeds to validate the performance of the trained ANN model. At the second decision point, the model's acceptability is assessed. If the model is not acceptable, the process returns to the ANN architecture step for possible redesign and retraining. If the model is accepted, it is then considered ready for prediction. The trained and validated ANN model is now ready to be deployed for making predictions.
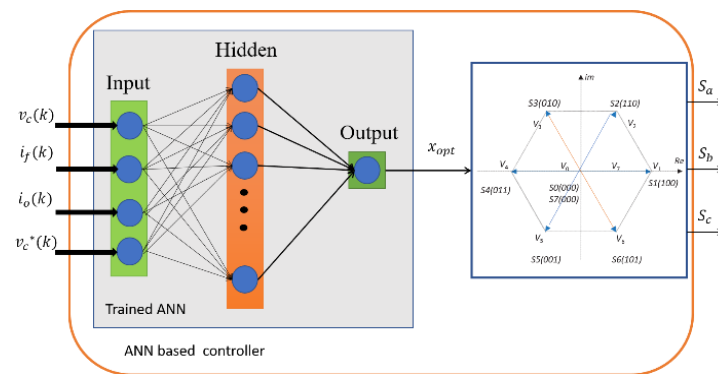

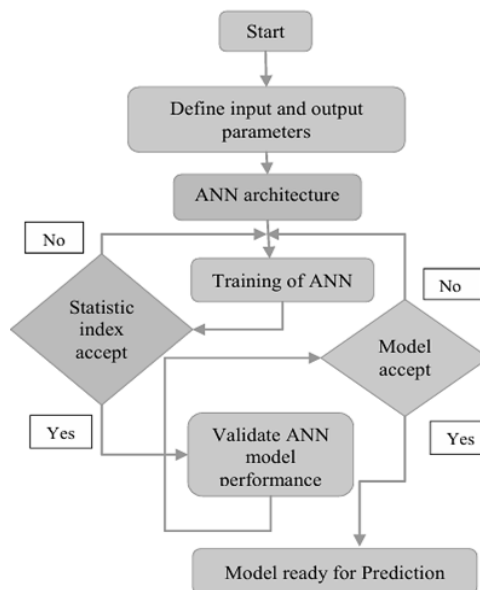Figure 6. Block diagram of the improved ANN-based controller

Figure 7. Flow chart of ANN modeling

3.   RESULTS AND DISCUSSION

In this section, we validate and compare the performance of the proposed ANN-MPC against FCS-MPC. This evaluation encompasses different loads and as well as different operating conditions. The system parameters used in the simulations are detailed in Table 1. Figure 8 shows the steady-state behavior of the ANN-based controller under a 50 Ω resistive load, while Figure 9 presents the response of the MPC under the same conditions. In Figures 8 and 9, the reference voltage is maintained at an amplitude of 200 V and a fundamental frequency of 50 Hz. The total harmonic distortion obtained by the ANN-based controller scheme is 0.39% for a resistive load of 50 Ω, have been depicted in Figure 10, and the total harmonic distortion obtained by the FCS-MPC scheme is 0.52% for a resistive load of 50 Ω, have been depicted in Figure 11.

Table 1. Converter system parameters

Parameter	Value
DC link voltage Vdc	500 V
Voltage reference	200 V
Filter capacitor C	50e-6 F
Filter inductance L	3.5e-3 H
Filter resistor	R/10 Ω
Reference frequency	50 fm
Sampling time Ts	10e-6 s
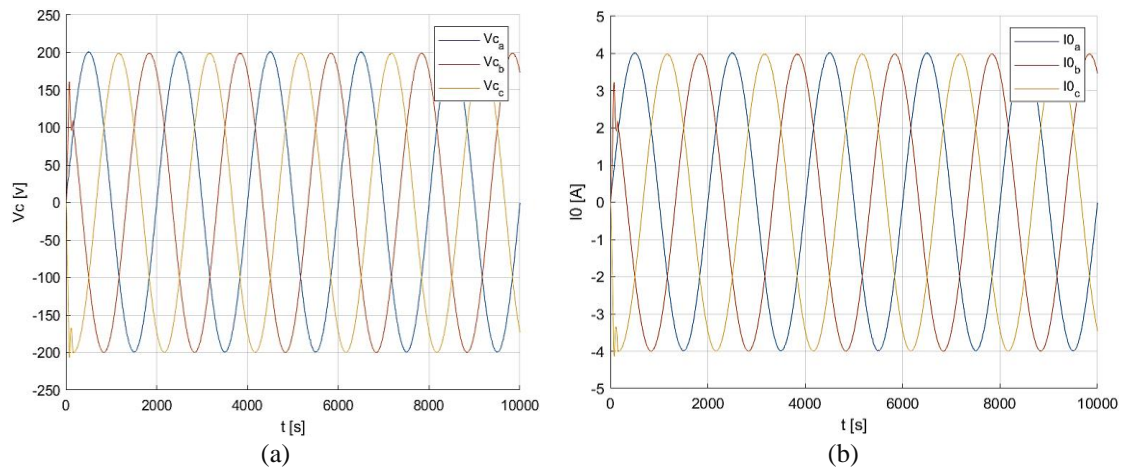
Figure 8. Simulated (a) output voltage and (b) output current for a 50 Ω resistive load controlled by the ANN-based scheme
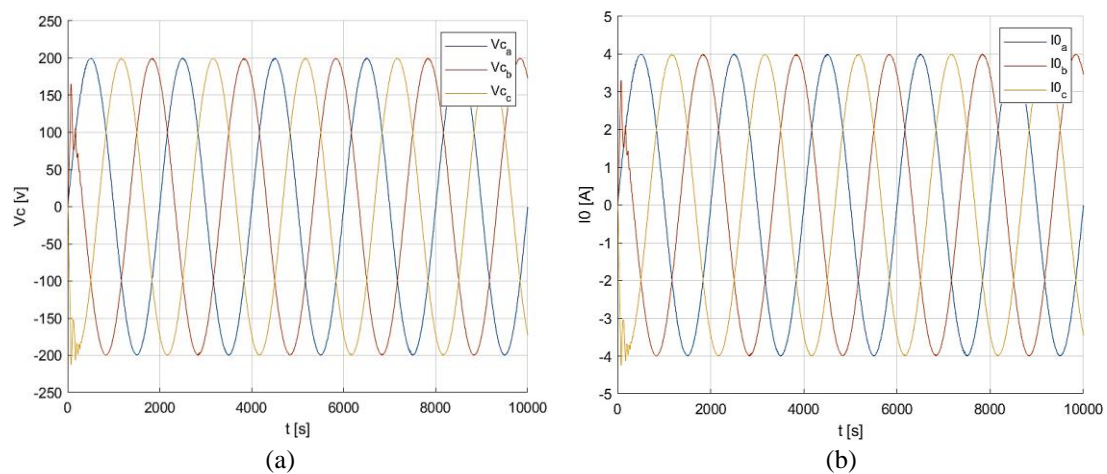

Figure 9. Simulated (a) output voltage and (b) output current, for a 50 Ω resistive load controlled by the FCS-MPC-based scheme

The plotted waveforms clearly demonstrate that both control strategies produce sinusoidal output voltages vcv_cvc with minimal distortion. Notably, the ANN-based controller achieves a lower total harmonic distortion (THD) of 0.39%, compared to 0.52% obtained using the conventional MPC approach. Furthermore, since the load is purely resistive, the output current i_0 is directly proportional to the output voltage. It is also observed that the filter current i_f, measured at the converter's output, contains high-frequency harmonics more prominent in the case of MPC, which are effectively attenuated by the RLC filter. Table 2 summarizes the simulation results for different resistive load values under both control strategies. Figures 12 and 13 illustrate the transient response of the ANN-MPC and FCS-MPC control schemes, respectively, under no load (i.e., open circuit).

The great dynamic performance of the suggested control technique is highlighted by the ANN-based controller's quick and steady transient response. In contrast, the MPC approach takes approximately 13 ms to reach a stable steady-state and accurately track the reference waveform. On the other hand, the ANN-based controller achieves the same stable state and tracks the reference waveform in less than 5 ms, demonstrating its superior dynamic response performance. The dynamic response to the increase in the amplitude of the reference voltage from 200 to 150 V at t = 0.045 s is presented in Figures 14 and 15 for the FCS-MPC and ANN-MPC methods, respectively.

Table 2. Summary of simulation results for various resistive load values

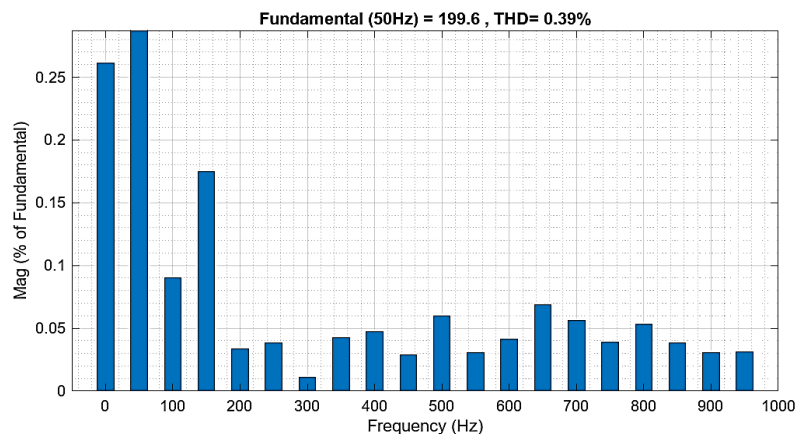| Resistor Ω	ANN-based controller THD%	FCS-MPC THD%
10	0.35	0.39
50	0.39	0.52
100	0.36	0.63
300	0.55	0.87

Figure 10. Total harmonic distortion obtained by ANN-based controller scheme
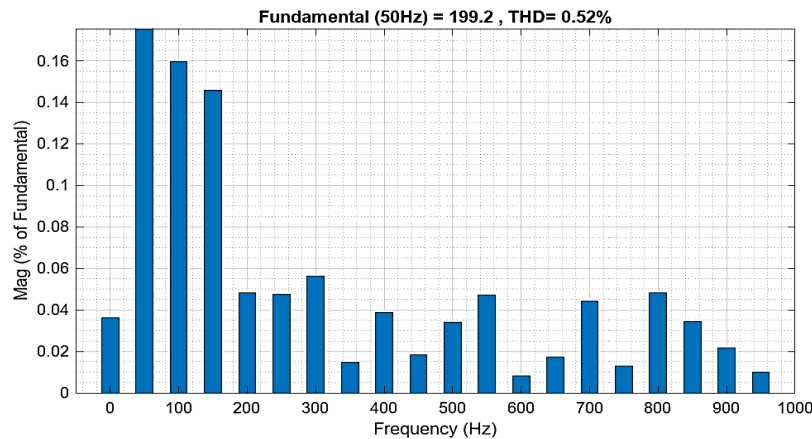

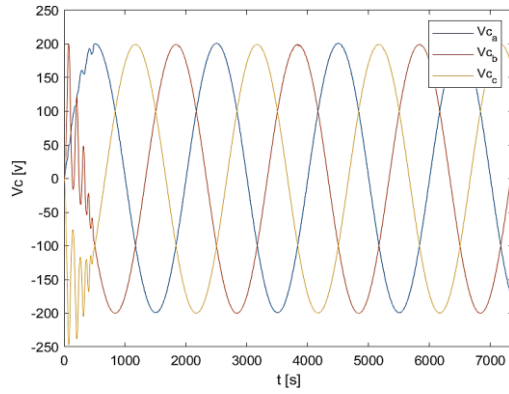Figure 11. Total harmonic distortion obtained by FCS-MPC scheme

Figure 12. The ANN-based controller's dynamic response when there is no load
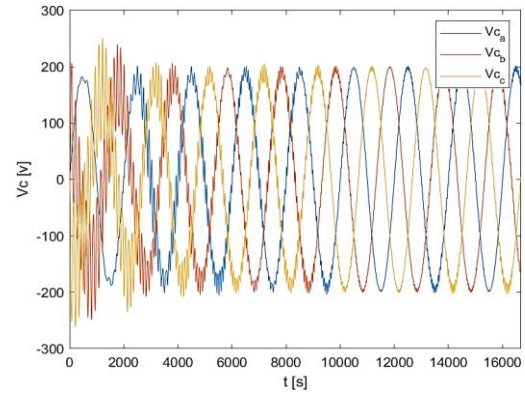

Figure 13. The dynamic response of the FCS-MPC-based controller when there is no load

In the ANN-MPC model, the system responds to a change in the input reference in less than 1 ms, while the traditional MPC system takes approximately 3 ms to react. This difference is due to the varying computational demands of the MPC model. To evaluate the practicality and performance of the proposed ANN-based controller under real-world conditions, we conduct online tests with nonlinear loads, such as a diode bridge rectifier, as illustrated in Figure 16. Figure 17 shows the output voltage of the ANN-based controller under a nonlinear load, while Figure 18 presents the response of the predictive controller under the same conditions. In both cases, the reference voltage is maintained at an amplitude of 150 V and a fundamental frequency of 50 Hz.
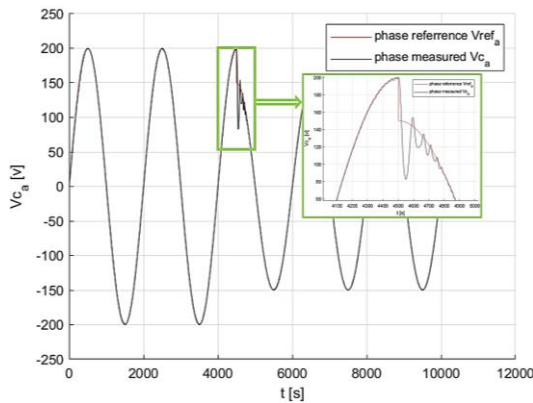

Figure 14. FCS-MPC-based control strategy's dynamic response: output voltage at t = 0.045 s when the reference voltage shifts from Vref = 200 V to Vref = 150 V
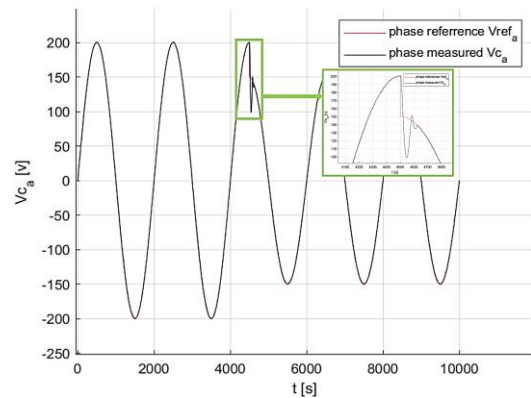

Figure 15. ANN-based control strategy's dynamic response: output voltage at t = 0.045 s when the reference voltage shifts from Vref = 200 V to Vref = 150 V
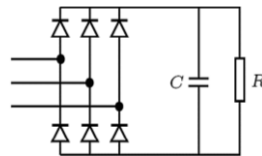

Figure 16. Non-linear model used with values C = 300 µF and R = 60 Ω

The data from the graphs demonstrate that the output voltage generated by the artificial neural network (ANN)-based controller outperforms that obtained with model predictive control (MPC) for nonlinear loads. To improve MPC's performance in this scenario, it would be advantageous to consider

implementing a shorter sampling time or adjusting the values of capacitance or filtering resistance upwards. The THD values given by the system for different resistance and capacitance values are shown in Table 3.
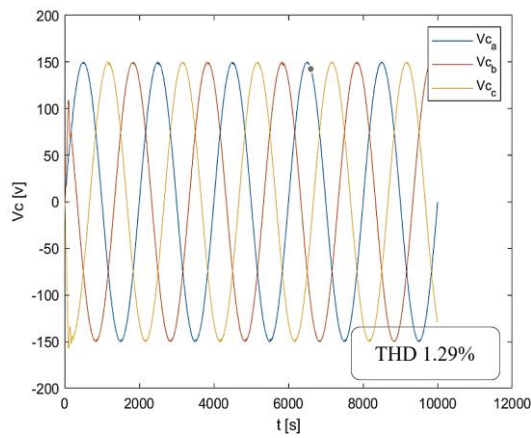

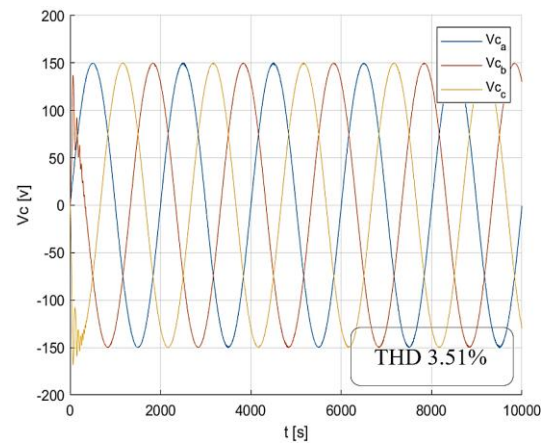Figure 17. Simulation results: output voltages (v_c [v]) for the ANN-MPC a C = 30 µF and R = 60 Ω

Figure 18. Simulation results: output voltages (v_c[v]) for the FCS-MPC a C = 30 µF and R = 60 Ω

Table 3. A summary for different values of non-linear load

Nonlinear loads C(µF) and R(Ω)	ANN-based controller THD%	FCS-MPC THD%
C = 30, R = 60	1.29	3.51
C = 30, R = 150	0.9	3.11
C = 100, R = 60	2.10	3.62
C = 100, R = 150	1.80	3.75

4. CONCLUSION

This study introduces an ANN-based MPC design for power converters with an output RLC filter. By combining the strengths of machine learning with the precision of MPC, this approach provides a comprehensive solution to the computational challenges associated with traditional MPC methods. Simulation results on three-phase converters demonstrate that the ANN-MPC approach maintains the control efficacy of conventional MPC while significantly reducing computational complexity. The neural network-based control strategy delivers a rapid dynamic response, reduced harmonic distortion, improved output voltage quality, and superior management of nonlinear loads compared to traditional MPC models. Future research may focus on the practical implementation of this ANN-based controller in real-world applications.

FUNDING INFORMATION

AUTHOR CONTRIBUTIONS STATEMENT

This journal uses the Contributor Roles Taxonomy (CRediT) to recognize individual author contributions, reduce authorship disputes, and facilitate collaboration.

Name of Author	C	M	So	Va	Fo	I	R	D	O	E	Vi	Su	P	Fu
Iftissen Nabil	✓	✓	✓	✓	✓	✓		✓	✓	✓	✓			
Ali Dali	✓	✓		✓			✓			✓	✓	✓		
Samir Abdelmalek	✓	✓		✓			✓			✓	✓	✓	✓	✓

C : **C**onceptualization	I : **I**nvestigation	Vi : **Vi**sualization
M : **M**ethodology	R : **R**esources	Su : **Su**pervision
So : **So**ftware	D : **D**ata Curation	P : **P**roject administration
Va : **Va**lidation	O : Writing - **O**riginal Draft	Fu : **Fu**nding acquisition
Fo : **Fo**rmal analysis	E : Writing - Review & **E**diting	

CONFLICT OF INTEREST STATEMENT
Authors state no conflict of interest.

DATA AVAILABILITY
The data that support the findings of this study are available from the corresponding author, [IN], upon reasonable request.

REFERENCES

[1]   Y. Abdel-Rady Ibrahim Mohamed and E. F. El-Saadany, "An improved deadbeat current control scheme with a novel adaptive self-tuning load model for a three-phase PWM voltage-source inverter," *IEEE Transactions on Industrial Electronics*, vol. 54, no. 2, pp. 747–759, Apr. 2007, doi: 10.1109/TIE.2007.891767.

[2]   P. Cortes, M. P. Kazmierkowski, R. M. Kennel, D. E. Quevedo, and J. Rodriguez, "Predictive control in power electronics and drives," *IEEE Transactions on Industrial Electronics*, vol. 55, no. 12, pp. 4312–4324, Dec. 2008, doi: 10.1109/TIE.2008.2007480.

[3]   Y. Han, G. He, X. Fan, Q. Zhao, and H. Shen, "Design and analysis of improved ADRC controller for multiple grid-connected photovoltaic inverters," *Modern Physics Letters B*, vol. 32, no. 34n36, p. 1740103, Dec. 2018, doi: 10.1142/S0217984918401036.

[4]   P. Prabhakaran, S. M. Krishna, D. J. L. Febin, and T. Perumal, "A novel PR controller with improved performance for single-phase UPS inverter," in *2021 4th Biennial International Conference on Nascent Technologies in Engineering (ICNTE)*, IEEE, Jan. 2021, pp. 1–6. doi: 10.1109/ICNTE51185.2021.9487688.

[5]   J. Li, Y. Sun, X. Li, S. Xie, J. Lin, and M. Su, "Observer-based adaptive control for single-phase UPS inverter under nonlinear load," *IEEE Transactions on Transportation Electrification*, vol. 8, no. 2, pp. 2785–2796, Jun. 2022, doi: 10.1109/TTE.2022.3151759.

[6]   L. M. A. Caseiro, A. M. S. Mendes, and S. M. A. Cruz, "Cooperative and dynamically weighted model predictive control of a 3-level uninterruptible power supply with improved performance and dynamic response," *IEEE Transactions on Industrial Electronics*, vol. 67, no. 6, pp. 4934–4945, Jun. 2020, doi: 10.1109/TIE.2019.2921283.

[7]   C. Shen, Y. Shi, and B. Buckham, "Trajectory tracking control of an autonomous underwater vehicle using Lyapunov-based model predictive control," *IEEE Transactions on Industrial Electronics*, vol. 65, no. 7, pp. 5796–5805, Jul. 2018, doi: 10.1109/TIE.2017.2779442.

[8]   M. Liu, Y. Shi, and X. Liu, "Distributed MPC of aggregated heterogeneous thermostatically controlled loads in smart grid," *IEEE Transactions on Industrial Electronics*, vol. 63, no. 2, pp. 1120–1129, Feb. 2016, doi: 10.1109/TIE.2015.2492946.

[9]   H. Han and J. Qiao, "Nonlinear model-predictive control for industrial processes: an application to wastewater treatment process," *IEEE Transactions on Industrial Electronics*, vol. 61, no. 4, pp. 1970–1982, Apr. 2014, doi: 10.1109/TIE.2013.2266086.

[10]   H. Li and Y. Shi, "Network-based predictive control for constrained nonlinear systems with two-channel packet dropouts," *IEEE Transactions on Industrial Electronics*, vol. 61, no. 3, pp. 1574–1582, Mar. 2014, doi: 10.1109/TIE.2013.2261039.

[11]   M. Nauman and A. Hasan, "Efficient implicit model-predictive control of a three-phase inverter with an output LC filter," *IEEE Transactions on Power Electronics*, vol. 31, no. 9, pp. 6075–6078, Sep. 2016, doi: 10.1109/TPEL.2016.2535263.

[12]   H. Miranda, P. Cortes, J. I. Yuz, and J. Rodriguez, "Predictive torque control of induction machines based on state-space models," *IEEE Transactions on Industrial Electronics*, vol. 56, no. 6, pp. 1916–1924, Jun. 2009, doi: 10.1109/TIE.2009.2014904.

[13]   S. Hanke, S. Peitz, O. Wallscheid, J. Bocker, and M. Dellnitz, "Finite-control-set model predictive control for a permanent magnet synchronous motor application with online least squares system identification," in *2019 IEEE International Symposium on Predictive Control of Electrical Drives and Power Electronics (PRECEDE)*, IEEE, May 2019, pp. 1–6. doi: 10.1109/PRECEDE.2019.8753313.

[14]   L. Kang, J. Cheng, B. Hu, X. Luo, and J. Zhang, "A simplified optimal-switching-sequence MPC with finite-control-set moving horizon optimization for grid-connected inverter," *Electronics*, vol. 8, no. 4, p. 457, Apr. 2019, doi: 10.3390/electronics8040457.

[15]   I. Nabil, M. Hamza, A. Samir, and D. Ali, "Model predictive voltage control of uninterruptible power supply with an output RLC filter," in *2023 2nd International Conference on Electronics, Energy and Measurement (IC2EM)*, IEEE, Nov. 2023, pp. 1–6. doi: 10.1109/IC2EM59347.2023.10419462.

[16]   X. Yin and X. Zhao, "Deep neural learning based distributed predictive control for offshore wind farm using high-fidelity LES data," *IEEE Transactions on Industrial Electronics*, vol. 68, no. 4, pp. 3251–3261, Apr. 2021, doi: 10.1109/TIE.2020.2979560.

[17]   D. S. Sarali, V. A. I. Selvi, and K. Pandiyan, "An improved design for neural-network-based model predictive control of three-phase inverters," in *2019 IEEE International Conference on Clean Energy and Energy Efficient Electronics Circuit for Sustainable Development (INCCES)*, IEEE, Dec. 2019, pp. 1–5. doi: 10.1109/INCCES47820.2019.9167697.

[18]   I. S. Mohamed, S. Rovetta, T. D. Do, T. Dragicevic, and A. A. Z. Diab, "A neural-network-based model predictive control of three-phase inverter with an output LC filter," *IEEE Access*, vol. 7, pp. 124737–124749, 2019, doi: 10.1109/ACCESS.2019.2938220.

[19]   V. Degli-Esposti *et al.*, "IEEE access special section editorial: Millimeter-wave and terahertz propagation, channel modeling, and applications," *IEEE Access*, vol. 9, pp. 67660–67666, 2021, doi: 10.1109/ACCESS.2021.3076326.

[20]   D. Wang *et al.*, "Model predictive control using artificial neural network for power converters," *IEEE Transactions on Industrial Electronics*, vol. 69, no. 4, pp. 3689–3699, Apr. 2022, doi: 10.1109/TIE.2021.3076721.

[21]   X. Liu, L. Qiu, Y. Fang, Z. Peng, and D. Wang, "Finite-level-state model predictive control for sensorless three-phase four-arm modular multilevel converter," *IEEE Transactions on Power Electronics*, vol. 35, no. 5, pp. 4462–4466, May 2020, doi: 10.1109/TPEL.2019.2944638.

[22]   F. Simonetti, A. D'Innocenzo, and C. Cecati, "Neural network model-predictive control for CHB converters with FPGA implementation," *IEEE Transactions on Industrial Informatics*, vol. 19, no. 9, pp. 9691–9702, Sep. 2023, doi: 10.1109/TII.2023.3233973.

[23]   M. Novak, T. Dragicevic, and F. Blaabjerg, "Weighting factor design based on artificial neural network for finite set MPC operated 3L-NPC converter," in *2019 IEEE Applied Power Electronics Conference and Exposition (APEC)*, IEEE, Mar. 2019, pp. 77–82. doi: 10.1109/APEC.2019.8722062.

[24] X. Yang, X. Liu, Z. Zhang, C. Garcia, and J. Rodriguez, "Two effective spectrum-shaped FCS-MPC approaches for three-level neutral-point-clamped power converters," in *2020 IEEE 9th International Power Electronics and Motion Control Conference (IPEMC2020-ECCE Asia)*, IEEE, Nov. 2020, pp. 1011–1016. doi: 10.1109/IPEMC-ECCEAsia48364.2020.9367780.

[25] K. Wang, X. Yang, S. Chen, and K.-B. Park, "FCS-MPC based dual-module ANN controller for three-level converter," in *2023 11th International Conference on Power Electronics and ECCE Asia (ICPE 2023 - ECCE Asia)*, IEEE, May 2023, pp. 1861–1866. doi: 10.23919/ICPE2023-ECCEAsia54778.2023.10213864.

BIOGRAPHIES OF AUTHORS

Iftissen Nabil obtained his Bachelor's degree in Electronics and his master's degree in instrumentation electronics in 2018 and 2020, respectively, from Abderrahmane Mira University of Béjaïa, Algeria. Since 2021, he has been a doctoral researcher at Médéa University, Algeria. His research focuses on model predictive control (MPC), power electronics, robotics, computer vision, and artificial intelligence. He can be contacted at email: iftissen.nabil@univ-medea.dz.

Ali Dali was born in Hussein Dey, Algeria, in 1986. He received his engineer's degree in automatic and electrical engineering from the Department of Automation, École Nationale Polytechnique of Algiers, Algeria, in 2009 and his Ph.D. degree in electrical engineering in 2021 from the same department. He has been an associate researcher at the Renewable Energy Development Center (CDER), Algeria, since 2013. His current research interests include nonlinear control, optimization techniques, and identification, as well as hybrid renewable energy systems. He can be contacted at email: a.dali@cder.dz.

Samir Abdelmalek was born in Tebessa, Algeria, in 1986. He received both his Engineer's degree and Magister's degree in Automatic and Electrical Engineering from the Department of Electrical Engineering at Echahid Cheikh Larbi Tebessi University, Tebessa, Algeria, in 2009 and 2012, respectively. He earned his Ph.D. in Electrical Engineering from USTHB (University of Science and Technology Houari Boumediene) in 2016. Currently, he is a full Professor in the National School of Nanoscience and Nanotechnology, Sidi Abdellah, Algiers, Algeria. His research interests include linear and nonlinear control systems, modern optimization techniques, and artificial intelligence applications in hybrid renewable energy systems. He can be contacted at email: s.abdelmalek@ensnn.dz.